This is the Pre-Published Version.

The following publication Q. F. Lin, S. X. Niu and T. T. Sheng, "Novel biased flux machine with double salient structure," 2016 Eleventh International Conference on Ecological Vehicles and Renewable Energies (EVER), 2016 is available at https://doi.org/10.1109/EVER.2016.7476409.

Novel Biased Flux Machine with Double Salient Structure

Q.F. Lin, S.X. Niu, Tian.Tian. Sheng
Department of Electrical Engineering, Hong Kong Ploytechnic University
E-mail: guaizhang.lin@polyu.edu.hk

***Abstract*—This paper presents a novel biased flux machine with an exterior rotor and a sailient stator with permanent magnets(PMs) and armature windings embedded in. The electromagnetic characteristics of this machine are analyzed under open-circuit and on-load conditions. Since the novel machine has a similar flux path with dc-excited flux-switching machine(DCE-FSM), a quantitative comparison study of these two machines, especially on the electromagnetic torque is conducted. The torque of the novel machine is relatively higher. The characteristics of the novel machine are simulated with 2-D time-stepping finite element method (TS-FEM).**

Keywords*—*biased flux, double salient, exterior rotor, permanent-magnet-stator, 2-D time-stepping finite element method

I. INTRODUCTION

Electric vehicles (EVs) consuming clean and low energy have drawn more and more attentions in recent days [1]. As a key part of EVs, motor drive has attracted a lot of attention. The basic characteristics which are required of EV motors are high torque density and high power density, wide speed range over constant power operating, high efficiency over wide speed and torque ranges [2]. Many researches have been done to investigate motors with various structures to fulfill these requirements.

Among these structures, double salient machine presents the advantages of high torque density and efficiency, simple and robust structure, high speed capability and low torque ripple [3]. Some improvements have been investigated in [4] and [5] by applying exterior rotor and partitioned stator and both of them show a relatively high torque density. Besides, in [6-8], it is also verified the stator permanent magnet (PM) machine exhibits a higher torque, lower torque ripple and more sinusoidal back-EMF characteristic and the thermal problem can be ease. And in [7] and [9], it is proved the selection of rotor poles of flux-biased machine is more flexible and the flux path of the flux-biased machine is shorter when compared with other double salient machines. And the three phase unbalance is overcame in the flux biased machine since the flux path of each phase in the stator is identical and balanced [7]. Moreover, the torque ripple of the flux-biased machine is smaller which is also preferable for EV applications.

In this paper, a novel machine with 24/20 stator/rotor poles is proposed aiming to integrate the advantages of double salient, stator PM, exterior rotor and biased flux machines within one machine. Firstly, the structure and winding distribution will be introduced and the operation principles and concept of biased flux will be discussed. Then, the electromagnetic characteristics of the proposed machine under open-circuit and on load condition will be simulated with time-stepping finite element method(TS-FEM) [10].

II. MACHINE CONSTRUCTION AND OPERATION PRINCIPLE

The proposed flux-biased double salient machine (BF-DSPMM) has compact and reliable structure with concentrated stator windings and double salient construction as shown in Fig. 1. The inner stator of this machine has 24 PM poles embedded in and each PM is magnetized in tangential direction having the opposite polarities with adjacent PMs. Some basic parameters of this machine are listed in Table I.

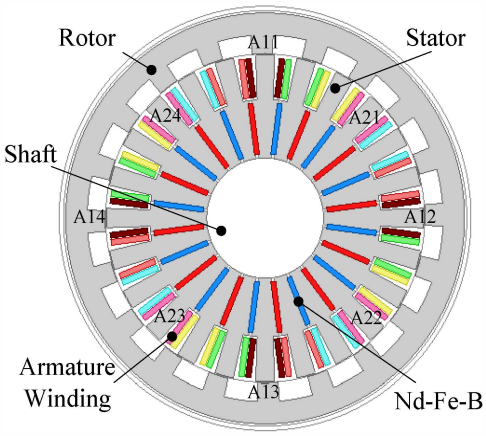

Fig. 1. Structure of the novel machine.

In Fig.1, the total coils are connected to form three phases, so each phase contains eight pairs of coils. Consequently the total flux linkage of one phase is affected by the eight pairs of coils and positions of salient poles of rotor. A11 to A24 represent the eight pairs of concentrated coils of Phase A. In order to obtain biased

©2016 IEEE. Personal use of this material is permitted. Permission from IEEE must be obtained for all other uses, in any current or future media, including reprinting/republishing this material for advertising or promotional purposes, creating new collective works, for resale or redistribution to servers or lists, or reuse of any copyrighted component of this work in other works.

magnetic flux-linkage, A11 to A14 are connected as group A1, and A21 to A24 are connected as group A2.

TABLE I
DESIGN SPECIFICATIONS OF THE PROPOSED MOTOR

Items	Value
Stator slot number	24
Rotor pole number	20
Active axial length	65 mm
Rotor outer radius	67 mm
Stator outer radius	53.5 mm
Rated speed	800 rpm
Air gap length	0.5 mm
Packing factor	0.5
Lamination Steel	XG196/96
Split ratio	0.59
Stator pole arc	15°
Rotor pole arc	18°
Turns per AC coil	30
Current density	5A/(mm)^2
PM thickness	1.68 mm
PM width	16.8 mm
PM permeability	1

The selection of stator and rotor poles should be satisfied the equations (1) and (2) [9]. The selection of rotor poles becomes more flexible since j can be any integer except which makes Nr equals to mk.

$$N_s = 2mk \tag{1}$$

$$N_r = N_s \pm j \ (N_r \neq mk) \tag{2}$$

where N_s is the number of stator poles, N_r is the number of rotor poles, m is the phase number, k and j are integers.

The basic operation mechanism of the proposed machine is shown in Fig.2. When one rotor pole moves from unaligned position to aligned position, the air-gap field will be enhanced since the positive current inject into armature coil to produce the same polarity flux with that of PM, thus positive torque is generated. On the contrary, when the rotor moves from aligned to unaligned position, negative current is injected into armature coil to weaken the air-gap field to help moving the rotor smoothly, as shown in Fig. 2(b). Then, the torque is generated over one electric cycle and the further smooth output torque are generated as a combined result of three phase operation.[7]

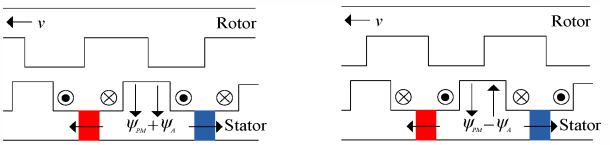

(a) (b)

Fig.2. Operation principle. (a) from unaligned position to aligned position. (b) from aligned position to unaligned position.

III. ELECTROMAGNETIC PERFORMANCE

A. Open-Circuit Characteristics

TS-FEM is used to simulate the static and dynamic performance of this machine. Since the flux distribution is symmetric, only half of it is shown in Fig.3. When one defines the direction of the flux-linkage from stator to rotor is the positive direction and from the rotor to stator is negative, the flux-linkage of Phase A varies from the maximum value to the minimum corresponding to the variation of flux distribution. When the rotor rotates by a quarter of rotor pole arc, the flux distribution changes from Fig.3(a) to (b) with 90° of electric angle variation and the flux-linkage changes from the positive maximum to zero. Further, the negative maximum flux-linkage of Phase A is reached when the corresponding rotor position is as shown in Fig.3(c). Meanwhile, the minimum of flux-linkage of coils A1 and A2 are also obtained. And then the flux-linkage of phase A returns to zero at position shown in Fig.3(d) due to the value of flux-linkage through coils A1 and coils A2 is equal but with opposite direction. The flux-linkages are formulated as below.

$$\psi_{A1} = \psi_{11} + \psi_{12} + \psi_{13} + \psi_{14} \tag{3}$$

$$\psi_{A2} = \psi_{21} + \psi_{22} + \psi_{23} + \psi_{23} \tag{4}$$

$$\psi_A = \psi_{A1} + \psi_{A2} \tag{5}$$

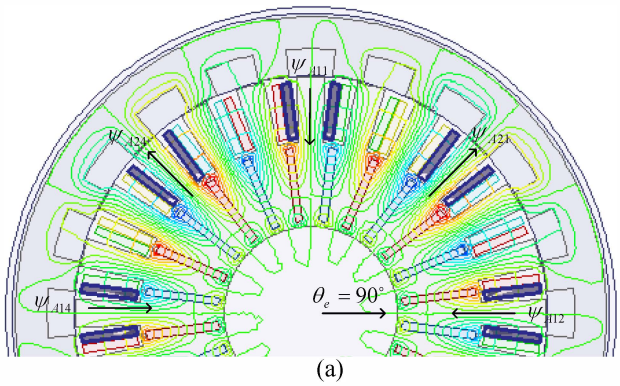

(a)

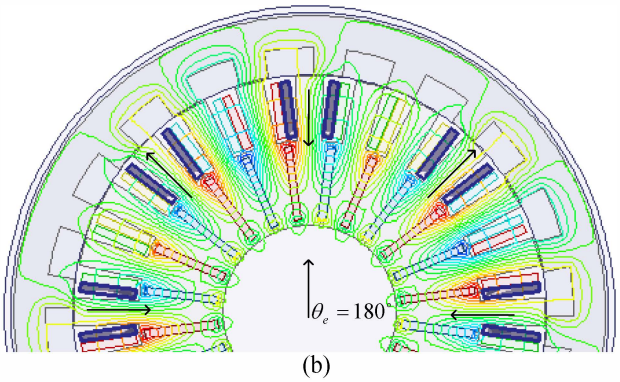

(b)

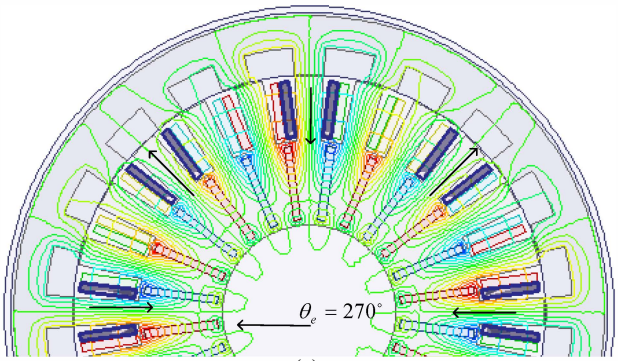

(c)

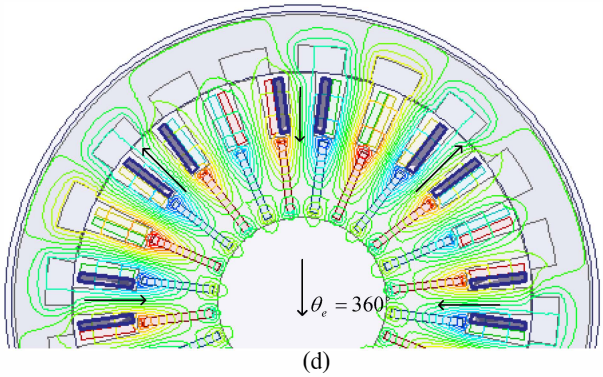

(d)

Fig.3. Open-circuit flux distribution of proposed machine. (a) θ_e=90º. (b) θ_e=180º. (c) θ_e=270º. (d) θ_e=360º .

The flux-linkage waveforms of Phase A in the proposed machine, including coil A1 and A2 are shown in Fig.4. The flux-linkage of A1 and A2 alone are unipolar and with 180 electrical degrees shifting due to the stator and rotor poles combination. However, the flux-linkage of phase A is bipolar and nearly sinusoidal which can be seen clearly from the fast Fourier Transform(FFT) result in Fig. 5. The biased flux-linkage is obtained accordingly.

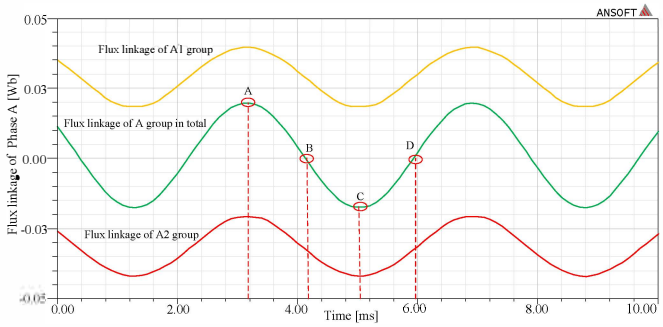

Fig.4. Flux linkage of Phase A.

As shown in Fig.5, there are DC components in coils A1 and A2 due to the flux leakage and the THDs are relatively higher. But the higher order harmonics of flux-linkage of phase A are relatively smaller for which the harmonics in coil A1 and A2 are canceled out with each other since they have nearly the same amplitude but half cycle difference of phase. This is also a common characteristic of the biased flux machine. And according to Eq. (6), the total harmonics distortion(THD) of Phase A is shown in Fig.5.

$$THD = 100\sqrt{\sum_{K=2}^{K} A_K^2 / (A_1 + \sum_{K=2}^{K} A_K^2)} \qquad (6)$$

where A_k is the amplitude of higher order harmonic, and A_1 is the amplitude of fundamental-wave.

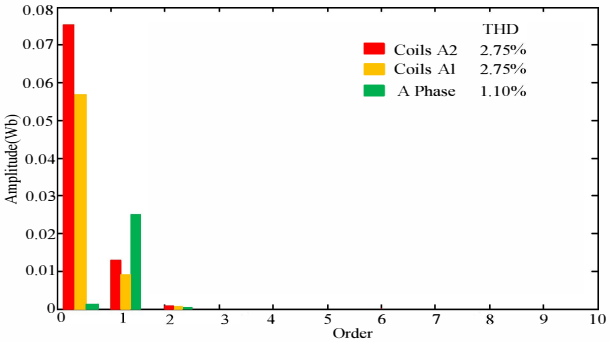

Fig.5. FFT analysis of flux linkage of Phase A.

The back-EMF waveforms of phase A including coil A1 and A2 with the current density *Je* equal to 5A/(mm)^2 at the rated speed of 800 rpm are shown in Fig.6(a). From the FFT result shown in Fig.6(b), it is shown that the induced back-EMF waveforms of coil A1 and A2 are asymmetric and the THD values are higher, however, the waveform of Phase A are close to sinusoidal with lower harmonics due to the cancellation of the even harmonics of coils A1 and A2. This can also be seen clearly through the analysis of FFT result as shwon in Fig.6(b). In order to obtain symmetric induced back-EMF waveforms, the number of stator poles and rotor poles must satisfy,

$$\frac{N_s}{\mathrm{HCF}(N_s, N_r)} = even \quad number \qquad (7)$$

where N_s and N_r are stator and rotor pole number respectively. HCF is the higher common factor[12].

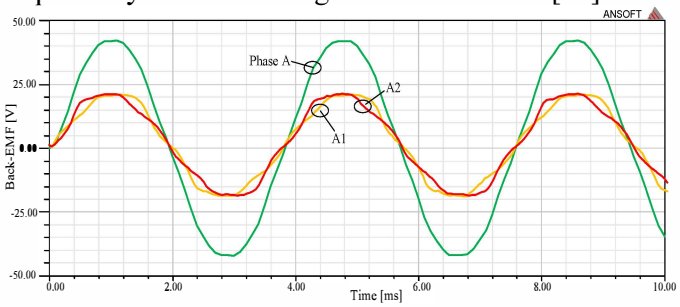

(a)

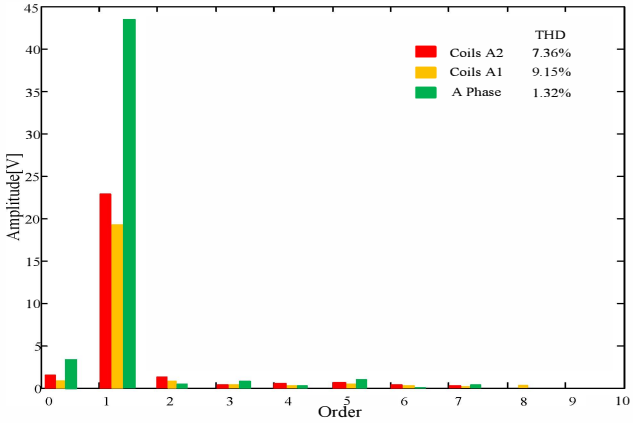

(b)

Fig.6. The Back-EMF of Phase A. (a)Back-EMF of Phase A, (b) analysis of Back-EMF of Phase A.

The cogging torque of the proposed machine is shown Fig.7(a). It can be observed that the cogging torque fluctuates cyclically. Through the FFT analysis result shown in Fig.7(b), it can be found that the 6th order harmonics are significant in the novel machine. This is different with the traditional machine with even number of rotor pole which has the 3rd and 6th significant harmonics. In conventional PM synchronous machines, the cogging torque is related with the goodness factor which is equal to 4 here[12].

$$C_T = \frac{N_r N_s}{N_c(N_s, N_r)} \qquad (8)$$

where C_T is the goodness factor of cogging torque, N_c is the common multiple.

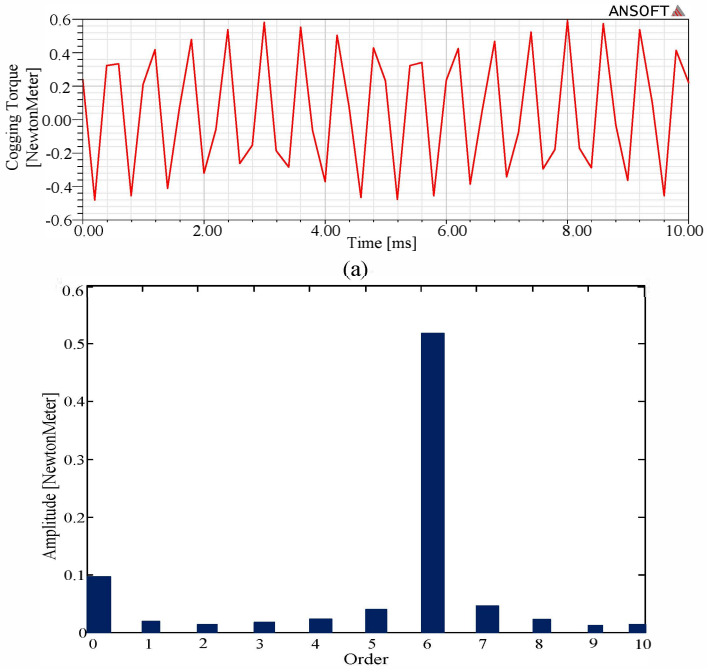

(a)

(b)

Fig.7. Cogging torque of the novel machine. (a) Cogging torque. (b) FFT analysis of the cogging torque.

B. *On-load Characteristics*

The output torque of the proposed machine is shown in Fig.8(a) with optimal current leading angle. Through the FFT analysis, it can be found that the fluctuations of torque are mainly caused by the 6th order harmonics, which also contributes to the cogging torque.

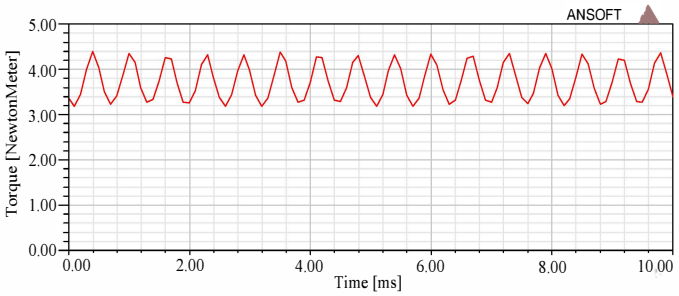

(a)

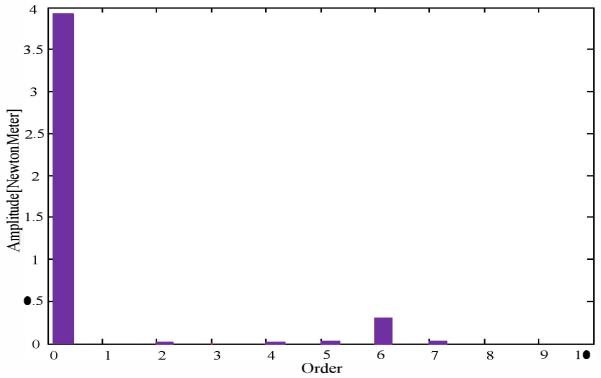

(b)

Fig.10. Torque characteristic of the proposed machine. (a) Electromagnetic torque. (b) FFT analysis of the electromagnetic torque.

Fig.11. shows the the average torque against the current leading angle at rated root-mean-square(RMS) current. It can be observed that the optimal input current leading angle of this novel machine is near 0^o. The torque doesn't start from zero due to the cogging torque and the flux path asymmetric.

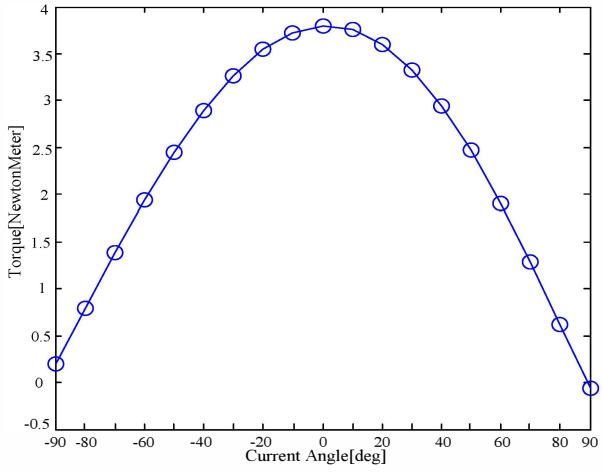

Fig.11. The output torque versus current angle at rated current.

The torque characteristic of the proposed machine is further investigated in comparison with a dc-excited flux-switching machine (DCE-FSM). This DCE-FSM has the same size and same structure of the proposed machine except that the Nd-Fe-B permanent magnets are replaced by DC coils. One stator tooth of the DCE-FSM is surrounded by a pair of DC concentrated coil. The structure of the DCE-FSM is shown in Fig.12.

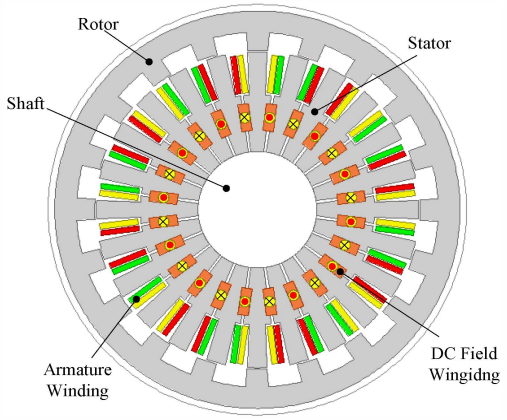

Fig.12. Structure of DCE-FSM machine

The phase armature current I_{ac}=0A and the DC field current density at the maximum value J_e=10A/(mm)^2 due to thermal problem and copper loss. The TS-FEM results of back-EMF of the DCE-FSM is shown in Fig.13. Compared with back-EMF of the proposed machine shown in Fig.6, it can be observed that back-EMF of the DCE-FSM is much smaller than the proposed machine. When comparing the torques of this two machines, it can be observed from Fig.14 that the torque produced by the proposed machine is nearly 3 times of the torque of DCE-FSM as shown in Fig.14. It is verified that the proposed machine has a much higher torque density than the DCE-FSM with the same structure and size. But the fluctuation of the torque of proposed machine is larger than the DCE-FSM due to the high flux-linkage density.

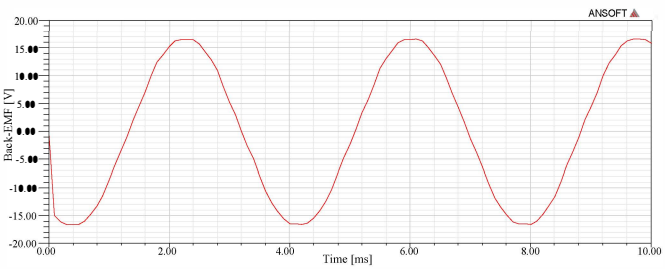

Fig.13. Back-EMF of Phase A of DCE-FSM

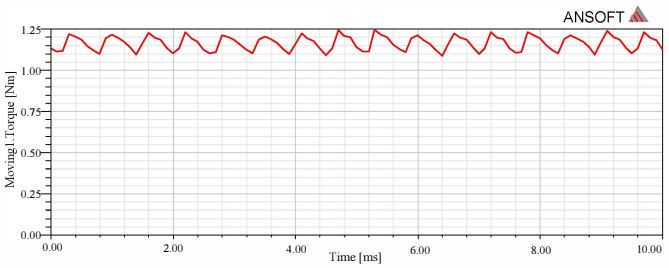

Fig.14. Torque waveform of DCE-FSM

IV. CONCLUSION

A biased flux machine with novel structure has been analyzed in this paper and some electromagnetic characteristics including flux-linkage, back-EMF, torque and the FFT analysis of these waveforms have been investigated. The biased-flux characteristic of the novel machine leads to highly sinusoidal waveforms with low harmonics. And the comparison with the DCE-FSM shows that the PMs excited field contributes to higher torque density and back-EMF which are more suitable to be applied in EVs .

V. REFERENCES

[1] C. C. Chan, *The state of the art of electric and hybrid vehicles*, Proc. IEEE,Vol. 90, No. 2, pp. 247 – 275, Feb. 2002.

[2] Z. Q. Zhu and D. Howe, *Electrical machines and drives for electric, hybrid, and fuel cell vehicles*, Proc. IEEE , Vol. 95, No. 4, pp. 746 – 765, April 2007.

[3] Y. Liao, F. Liang, and T. A. Lipo, *A novel permanent magnet motor with doubly salient structure,* IEEE Trans. Ind. Appl., Vol. 31, No. 5, pp. 1069 – 1078, Sep./Oct. 1995.

[4] Lei Gu, Fahimi, B., Kiani, M. and Wei WangA, *Novel High Energy Density Double Salient Exterior Rotor Permanent Magnet Machine*, IEEE Trans. on Magn., Vol.51, No.3, Mar., 2015.

[5] Wu, Z. Z., Zhu, Z. Q., Shi, J. T, *Novel Doubly Salient Permanent Magnet Machines With Partitioned Stator and Iron Pieces Rotor*, IEEE Trans. on Magn., Vol.51, No.5, pp.1-12, May 2015.

[6] Jianzhong Zhang, Ming Cheng, Zhe Chen and Wei Hua, *Comparison of Stator-Mounted Permanent-Magnet Machines Based on a General Power Equation*, IEEE Trans. on Energy Conversion, Vol.24, No.4, pp.826-834, Dec. 2009.

[7] Shi, J. T, Zhu, Z. Q., Wu, D. and X. Liu, *Comparative Study of Novel Synchronous Machines Having Permanent Magnets in Stator Poles*, Electrical Machines (ICEM), 2014 International Conference on, pp.429-435, Sept. 2014.

[8] Chunhua Liu, Chau, K.T., Jiang, J.Z., Niu, S., *Comparison of Stator-Permanent-Magnet Brushless Machines,* IEEE Trans. on Magn., Vol.44, No.11, pp.4405-4408, Nov. 2008.

[9] Shi, J. T, Zhu, Z. Q., Wu, D. and X. Liu, *Comparative Study of Novel Biased Flux Permanent Magnet Machine with Doubly Salient Permanent Magnet Machine,* Electrical Machines and Systems (ICEMS), 2014 17th International Conference on, pp.415-420, Sept. 2014.

[10] S. Niu, S. L. Ho, and W. N. Fu, *Power balanced electromagnetic torque computation in electric machines based on energy conservation in finite-element method*, IEEE Trans. on Magn., Vol.49, No.5, pp.2385-2388, May 2013.

[11] Z. Q. Zhu, and David Howe, *Influence of design parameters on cogging torque in permanent magnet machines,* IEEE Trans. on Energy Convers., Vol. 15, No. 4, pp. 407-412, Dec. 2000.

[12] Awah, C.C., Zhu, Z.Q., Wu, Z., and Wu, D., *High torque density magnetically-geared switched flux permanent magnet machines,* Ecological Vehicles and Renewable Energies (EVER), 2015 Tenth International Conference on, pp. 1-6, Mar. 2015.

[13] Y. Tang, J. J. H. Paulides, T. E. Motoasca, and E. A. Lomonova, *Flux-switching machine with DC excitation,* IEEE Trans. On Magn., Vol.48, No.11, pp.3583-3585, Nov. 2012.

[14] J. T. Shi, X. Liu, D. Wu, and Z. Q. Zhu, *Influence of Stator and Rotor Pole Arcs on Electromagnetic Torque of Variable Flux Reluctance Machines,* IEEE Trans. on Magn., Vol.50, No.11, pp.1-4, Nov. 2014.